Stationary Vortices and Pair Currents in a Trapped Fermion Superfluid

P. Capuzzi, E. S. Hernández & L. Szybisz

Journal of Low Temperature Physics

ISSN 0022-2291

J Low Temp Phys
DOI 10.1007/s10909-014-1271-9

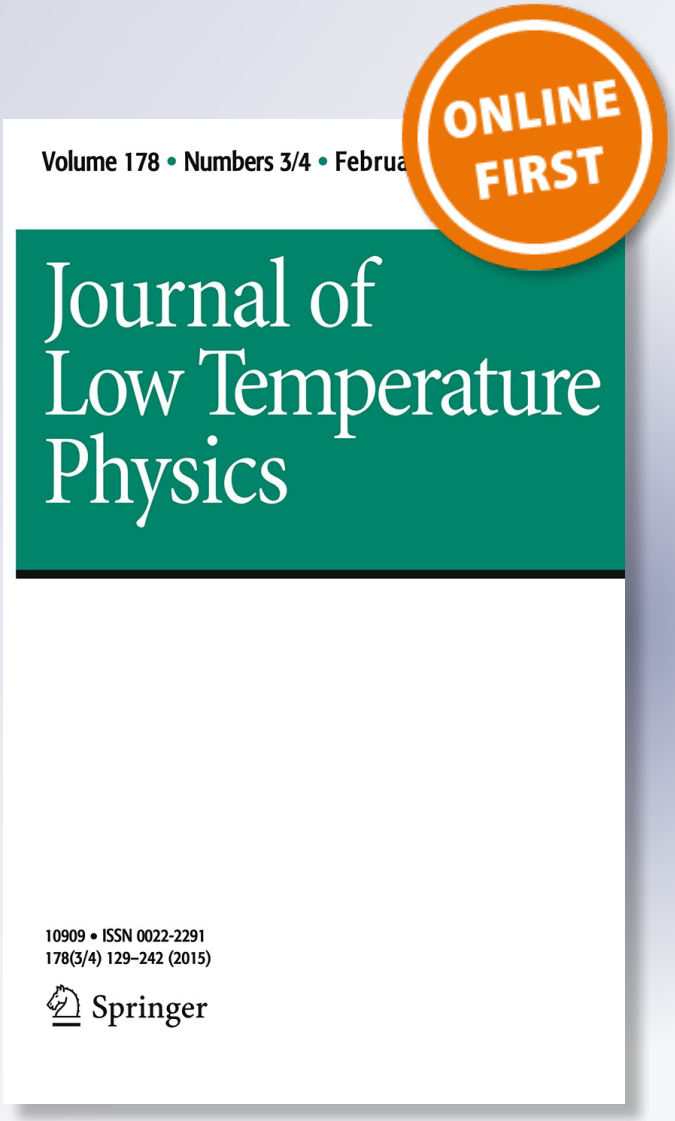

Springer

J Low Temp Phys
DOI 10.1007/s10909-014-1271-9

Stationary Vortices and Pair Currents in a Trapped Fermion Superfluid

P. Capuzzi · E. S. Hernández · L. Szybisz

Received: 13 February 2014 / Accepted: 30 December 2014

Abstract We examine the effects of stationary vortices in superfluid ^{6}Li atoms at zero temperature in the frame of the recently developed fluiddynamical scheme, that includes the pair density and its associated pair current and pair kinetic energy in addition to the fields appearing in the hydrodynamical description of normal fluids. In this frame, the presence of any particle velocity field gives rise to the appearance of a pair current. As an illustration, we consider a stationary vortex with cylindrical geometry in an unpolarized fluid, and examine the effects of the rotational velocity field on the spatial structure of the equilibrium gap and the profiles of the pair current. We show that the latter is intrinsically complex and its imaginary part is the source of a radial drift for the velocity field. We discuss the consequences on the stationary regime.

Keywords Trapped superfluid · Vortex · BCS–BEC

P. Capuzzi (✉) · E. S. Hernández · L. Szybisz
Departamento de Física, Facultad de Ciencias Exactas y Naturales, Universidad de Buenos Aires, Buenos Aires, Argentina
e-mail: capuzzi@df.uba.ar

P. Capuzzi · E. S. Hernández
Instituto de Física de Buenos Aires, Consejo Nacional de Investigaciones Científicas y Técnicas, Buenos Aires, Argentina

L. Szybisz
Consejo Nacional de Investigaciones Científicas y Técnicas, Buenos Aires, Argentina

L. Szybisz
Comisión Nacional de Energía Atómica, Buenos Aires, Argentina

Published online: 15 January 2015

1 Introduction

Quantized rotational flow is one the fundamental features of a superfluid, either bosonic or fermionic, as presented in numerous review papers and advanced textbooks (see e.g., Refs. [1–4]). The strictly quantum nature of superfluids and superconductors permits a quasiphenomenological description of superflow in terms of quantum hydrodynamics, where the superfluid velocity is the gradient of the phase of the particle wave function, and can thus support quantized circulatory motion. In the case of paired fermions, an important related issue that received attention in the past is the role of the orbital angular momentum density as a source of mass current density both in BCS superconductors and in anisotropic superfluids [5–9]. In the case of anisotropic ^{3}He–A, the intrinsic angular momentum originating in the orbital angular momentum of the Cooper pairs density can enter as a variable in the hydrodynamics of the nonuniform textures of helium [1,10].

It is well established that standard bosonic quantum hydrodynamics at zero temperature can be derived in the frame of a mean-field dynamics of the condensate wave function [11,12]. The superfluid density and velocity appear in the polar representation of such wave function. In the case of fermions, the simplest mean-field dynamical frame, the Hartree–Fock–Bogoliubov theory, leads to a system of coupled evolution equation for the particle density and pair density matrices [13,14]. A simple reduction of these two equations to their diagonal form as a first attempt to seek a description in terms of macroscopic fields immediately leads to the need of introducing a first moment of the particle density, namely the particle current. However, in order to close these three equations one has to introduce some nontrivial physical *ansatz* in the motion of the pair density [15]. The scheme exhibits then an important degree of ambiguity whose consequence is the impossibility of reaching an essential feature of the low energy spectrum of fermion superfluids, such as the existence of a gapped mode that represents oscillations in the pair density [16,17].

We have recently proven that this ambiguity can be removed, recovering the massive pairing mode in homogeneous [18,19] and trapped [20] superfluids by applying rigorously the criterion that gives rise to classical hydrodynamics. This consists of a derivation of coupled equations of motion for the first and second moments of both the particle and the pair density, prior to selecting the diagonal terms of the quantum matrices. This procedure gives rise to the fluiddynamical scheme (FD) formulated in terms of particle and pair densities, together with their current and kinetic energy densities, and is equivalent to keeping quantum mechanics up to order $\hbar^2$ in the full dynamics of the macroscopic fields. We have examined several aspects of equilibrium, stationary particle currents, and low energy dynamics; various numerical applications permit us to validate the usual local density approach (LDA) undertaken for the study of trapped fermions [21], also showing that the full FD description is needed to reach the low energy spectrum [15,18–20,22,23].

In the present work, we focus on one effect of the superfluid velocity field of a quantized vortex in a trapped fermion system at zero temperature. Comprehensive as well as introductory reviews to cold atomics physics that encompass basic aspects of laser cooling and trapping techniques with the corresponding developments can be found in Refs. [12,21,24–26]. Previous studies of rotational flow in ultracold

fermions have mainly focused on homogeneous systems resorting to the full solutions of Bogoliubov-de-Gennes equations [27–29]. On the other hand, we extend the FD procedure at zero temperatures employed in our earlier studies of FD to realize the LDA, in such a way that the local superfluid also carries a local translationally invariant flow. As shown in the forthcoming sections, large values of the local superfluid velocity such as those appearing at the vortex core suppress superfluidity giving rise to an unpaired, normal fluid. The FD equations of motion make evident that even in the stationary regime, such a current gives rise to a complex pair current, i.e., to a nonvanishing first moment of the pair density matrix— that might eventually destabilize the impressed vortex. We discuss the stability of the stationary regime in terms of the two-body interaction strength $\mathrm{g} = 4\pi\hbar^2 a/m$, with a the scattering length, and show that to a good approximation, even for not too low values of the latter, the flow remains stable and the particle density undergoes very slight modifications. Taking into account that the numerical solution of the FD scheme is far from trivial, we employ approximations of proven validity to provide insight on future developments.

This paper is organized as follows. In Sect. 2 we shortly review the FD formalism for a symmetric system of fermions in a harmonic trap and in Sect. 3, we derive the form of the pair current enslaved to a stationary linear vortex. We present and discuss numerical solutions in Sect. 4 and summarize our conclusions in Sect. 5.

2 The Fluiddynamical Equations

As is well known, the theory of fermion superfluids can be formulated in terms of a generalized density matrix that contains expectation values of products of two field operators $\Psi_\sigma^\dagger(\mathbf{r})$ and $\Psi_\sigma(\mathbf{r})$, namely

$$R_\sigma(\mathbf{r},\mathbf{r}') = \begin{pmatrix} \rho_\sigma(\mathbf{r},\mathbf{r}') & \kappa^*_{-\sigma}(\mathbf{r},\mathbf{r}') \\ -\kappa_\sigma(\mathbf{r},\mathbf{r}') & \delta(\mathbf{r}-\mathbf{r}') - \rho_{-\sigma}(\mathbf{r}',\mathbf{r}) \end{pmatrix}$$

with

$$\rho_\sigma(\mathbf{r},\mathbf{r}') = \langle\hat{\rho}_\sigma(\mathbf{r},\mathbf{r}')\rangle = \langle\Psi_\sigma^\dagger(\mathbf{r}')\Psi_\sigma(\mathbf{r})\rangle \tag{1}$$

for particle species with spin $\sigma = \pm$ and

$$\kappa_\sigma(\mathbf{r},\mathbf{r}') = \langle\Psi_\sigma(\mathbf{r})\Psi_{-\sigma}(\mathbf{r}')\rangle \tag{2}$$

for the pairing tensor. The FD (see e.g., Ref. [19] for a review) is formulated in terms of six coupled evolution equations for the particle density and pairing tensor and for their associated current and kinetic energy densities. The latter are the first two terms in a gradient expansion of the above matrices and read

$$\mathbf{j}_\sigma(\mathbf{r},\mathbf{r}') = \left\langle \frac{\hbar}{2m\imath}(\nabla - \nabla')\hat{\rho}_\sigma(\mathbf{r},\mathbf{r}') \right\rangle, \tag{3}$$

$$\tau_\sigma(\mathbf{r},\mathbf{r}') = \left\langle \frac{\hbar^2}{2m}\nabla\cdot\nabla'\hat{\rho}_\sigma(\mathbf{r},\mathbf{r}')\right\rangle \tag{4}$$

and correspondingly, $\mathbf{j}_\kappa$ and τ_κ defined as above with gradients operating upon $\kappa(\mathbf{r},\mathbf{r}')$ (hereafter we adopt the notation $\kappa \equiv \kappa_+$). The FD equations are obtained after computing the dynamical equations for the above six matrices and taking the limit for $\mathbf{r}\to\mathbf{r}'$. For an unpolarized fermion system with equal populations $N_\sigma = N/2$, they read

$$\frac{\partial\rho}{\partial t} = -\nabla\cdot\mathbf{j}, \tag{5}$$

$$\frac{\partial\mathbf{j}}{\partial t} = -\frac{\rho}{m}\nabla\mu + \frac{4\mathrm{g}}{\hbar}\mathrm{Im}(\kappa\mathbf{j}_\kappa^*), \tag{6}$$

$$\begin{aligned}\frac{\partial\tau}{\partial t} &= -\nabla\cdot\mathbf{j}_\tau - \nabla\left(2V+\mathrm{g}\rho\right)\cdot\mathbf{j}_\sigma + \frac{4\mathrm{g}}{\hbar}\mathrm{Im}(\kappa\tau_\kappa^*)\\ &\quad -4\mathrm{g}\mathrm{Re}\left(\mathbf{j}_\kappa^*\cdot\nabla\kappa\right) - \frac{4\mathrm{g}}{\hbar}\frac{\hbar^2}{2m}\mathrm{Im}(\kappa^*\nabla^2\kappa),\end{aligned} \tag{7}$$

$$\imath\hbar\frac{\partial\kappa}{\partial t} = \left(-\frac{\hbar^2}{4m}\nabla^2 + 2V - 2\mu_0\right)\kappa + 2\tau_\kappa, \tag{8}$$

$$\begin{aligned}\imath\hbar\frac{\partial\mathbf{j}_\kappa}{\partial t} &= \left(-\frac{\hbar^2}{4m}\nabla^2 + 2V + \mathrm{g}\rho - 2\mu_0\right)\mathbf{j}_\kappa - \mathrm{g}\mathbf{j}\kappa\\ &\quad + \lim_{s\to 0}\left(-\frac{\hbar^2}{m}\nabla_{\mathbf{s}}^2\mathbf{j}_\kappa\right),\end{aligned} \tag{9}$$

$$\begin{aligned}\imath\hbar\frac{\partial\tau_\kappa}{\partial t} &= \left(-\frac{\hbar^2}{4m}\nabla^2 + 2V + \mathrm{g}\rho - 2\mu_0\right)\tau_\kappa\\ &\quad -\mathrm{g}\tau\kappa - \frac{\hbar^2}{4m}\left[\nabla^2\left(2V+\mathrm{g}\rho\right)\kappa - \mathrm{g}\rho\nabla^2\kappa\right]\\ &\quad + \lim_{s\to 0}\left(-\frac{\hbar^2}{m}\nabla_{\mathbf{s}}^2\tau_\kappa\right)\end{aligned} \tag{10}$$

with ρ, $\mathbf{j}$, and τ representing the total densities, μ is the local chemical potential, μ_0 the chemical potential of both species and $V(\mathbf{r}) = m\omega^2 r^2/2$ the isotropic trapping potential of angular frequency ω.

It is to be noted [19] that the FD approach is not an alternative form for the two-fluid model of superfluids; at zero temperature, $\rho_+ + \rho_-$ is the superfluid density and in the absence of $\mathbf{j}_\kappa$, Eqs. (5) and (6) are the standard equations of superfluid hydrodynamics [21]. In previous works [15,18–20,22,23] we have proposed two criteria for approximations of the FD scheme that extend the standard LDA. The superfluid Thomas–Fermi approximation [15] (STF) consists of the set (5), (6), and (8) with the pair kinetic energy replaced by its expression for the homogeneous system, provided by the method of Ref. [30]. The extended superfluid Thomas–Fermi [19] (ESTF) approximation corresponds to considering the full set (5) to (10), replacing the explicit limits in the last two equations by their homogeneous expressions, obtained according

to a generalization of [30]. We have shown [19] that ESTF does not provide remarkable differences with respect to STF when structural features such as equilibrium densities and low energy spectra are considered; however, all moments of the above quantum matrices up to order $\hbar^2$, i.e., the current and kinetic energy densities, contemplated in the full ESTF, must be taken into account to obtain massive modes such as the pairing vibrations, that involve internal motion of the pairs [18–20].

Our present interest is to advance one more step on the understanding of currents and their interplay with the remaining fields, especially with the particle and the pair densities. We note that it is customary to find in the literature references to κ as the "pair density", overlooking the fact that it is a complex order parameter. In this philosophy, it is natural to refer to the corresponding first and second moments as pair current and pair kinetic energy as shorthands for pairing current tensor and pairing kinetic energy tensor. It should, however, be kept in mind that these are complex quantities that do not represent actual mass flow or energy content. We see that according to Eq. (9), any particle current $\mathbf{j}$ acts as a source of a pair current $\mathbf{j}_\kappa$. In what follows we illustrate the appearance of the latter and its consequences with a specific example.

3 The Pair Current in the Stationary Regime

We assume that a quantized superfluid velocity field

$$\mathbf{v}_\mathrm{s} = \frac{\hbar l}{mr}\hat{\varphi} \tag{11}$$

with $l = 0, \pm 1, \pm 2, \ldots$, corresponding to a linear vortex with circulation $\Gamma = hl/m$ has been impressed in the gap profile. In the spirit of an LDA, the stationary density is the solution of

$$\nabla\mu \equiv \nabla\left[\varepsilon_\mathrm{F}(\rho, v_\mathrm{s}) + V(\mathbf{r}) + \frac{\mathrm{g}\rho}{2}\right] = 0 \tag{12}$$

with $\varepsilon_\mathrm{F}(\rho, v_\mathrm{s})$ the Fermi energy of the homogeneous system with superfluid velocity $\mathbf{v}_\mathrm{s}$, computed from the total kinetic energy following Refs. [30,31]. The constant chemical potential μ_0 is set identical to the function in square brackets in Eq. (12) and its value is obtained by normalization of the density to the total number of particles.

Since particle and superfluid velocity fields differ in general—in particular, at the vortex core, which is populated by normal fluid—we have extended the ESTF to determine the particle current as well, on the same footing as the particle density. The procedure, that generalizes the ideas put forward in Ref. [30], consists in computing, in addition to those integrals that define the pairing gap and the particle density in the above paper, an integral for the current that derives from a velocity potential $\hbar\mathbf{q}\cdot\mathbf{r}/m$. The substitution of the velocity $\hbar\mathbf{q}/m$ by $\mathbf{v}_\mathrm{s}(r)$ in Eq. (11) permits to construct a local superfluid which, in addition to satisfying a local equation of state, carries a local translationally invariant flow. As shown in the Appendix, where we collect the main formulae, this calculation is far from trivial, in view of the angular dependence that

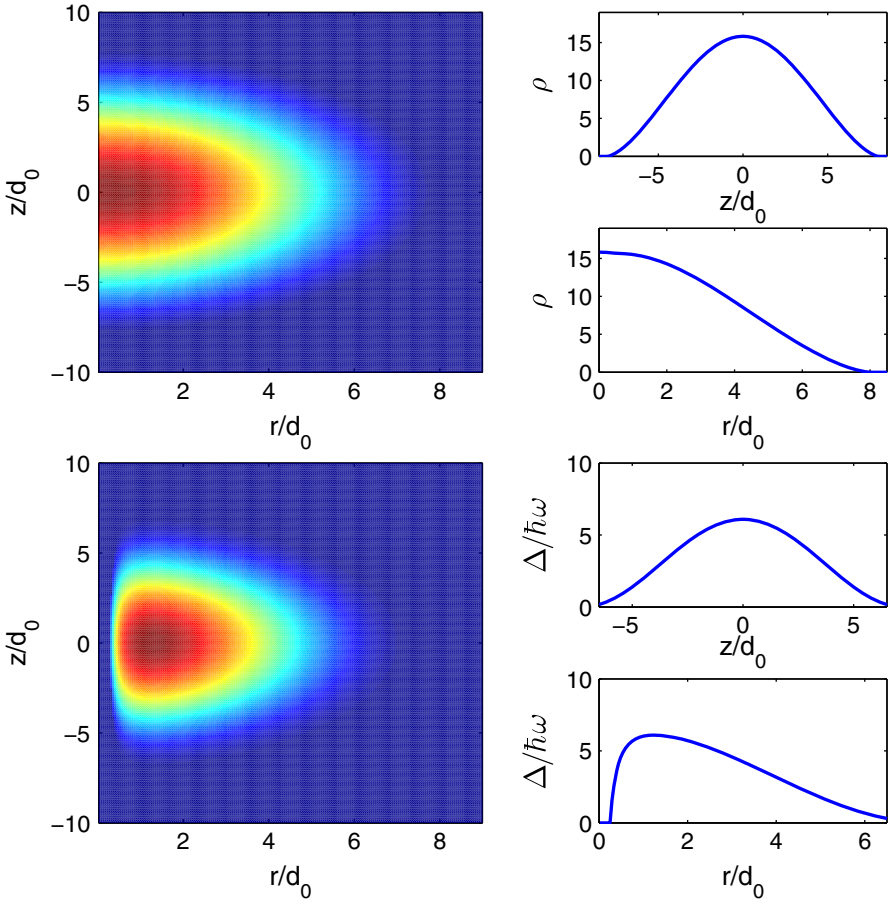

Fig. 1 Plots on the (r, z) plane for angular momentum $l = 1$. *Upper panel* particle density. *Lower panel* superfluid gap. Calculations are done in the LDA approximation. All spatial dimensions are given in units of the oscillator length $d_0 = \sqrt{\hbar/m\omega}$ (Color figure online)

the vector field introduces in the quasiparticle energy appearing in the integrands of Eqs. (38), (39), and (40).

We recall that the presence of a superfluid particle current reduces the gap amplitude [31]; moreover, the density profiles are sensitive to the centrifugal potential of the velocity field. Given the microscopic structure of the gap, it is reasonable to assume that the global velocity field incorporates a phase factor in each field operator $\Psi^\dagger, \Psi$. Consequently, for the pair density κ, we propose a vortex structure with twice the multipolarity of the velocity field, of the form

$$\kappa(r, z, \varphi) = e^{\imath 2l\varphi}\kappa(r, z). \tag{13}$$

This is illustrated in Figs. 1 and 2, where we show contour plots on the (r, z) plane for ρ and for the superfluid gap $\Delta = -g\kappa$ corresponding to $l = 1$ and 2, respectively. These

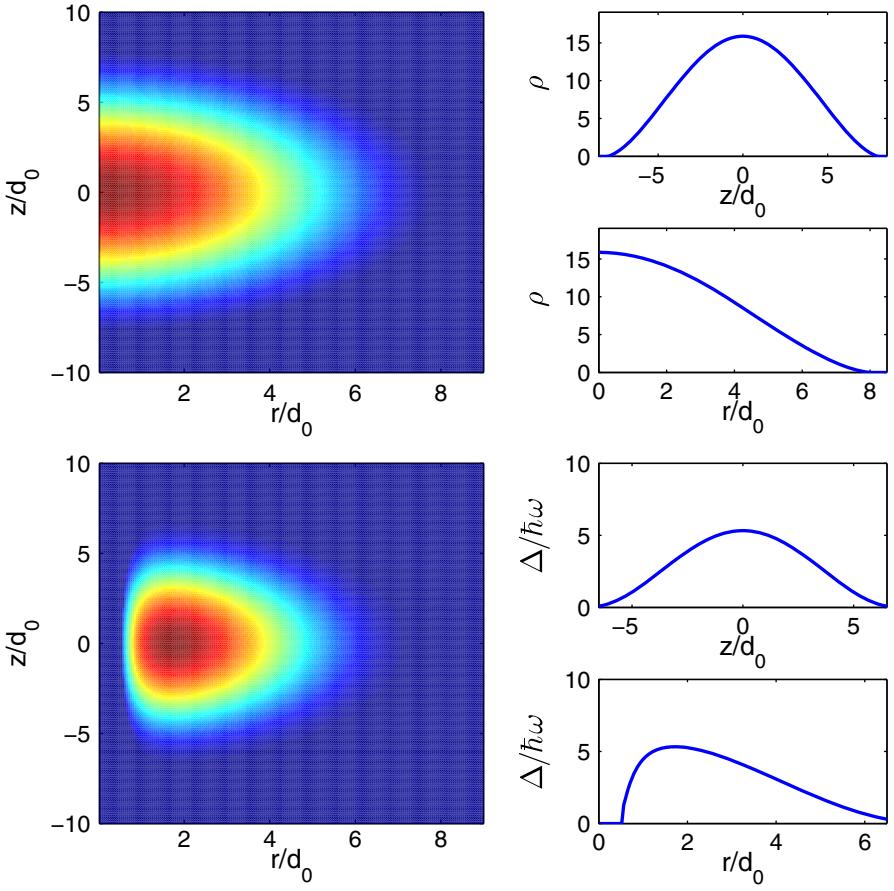

Fig. 2 Same as Fig. 1 for $l = 2$ (Color figure online)

calculations correspond to $N = 17{,}000$ ^{6}Li atoms in a spherical trap with frequency $\omega = 817$ Hz, interacting with scattering length $a = -114$ nm [32].

In Figs. 1 and 2 the density profile appears rather flat at the trap center without a strong effect of the presence of the vortex, however as we compare the density profiles for stronger interactions, we confirm that as we increase $|a|$ the gap and the superfluid fraction increase, and therefore the vortex centrifugal barrier excludes more and more atoms from the trap center, giving rise to a local depletion of the particle density. This is illustrated in Fig. 3 for $a = -114, -130$, and -140 nm.

The FD equations in the preceding section indicate that a stationary pair current sets in as the solution of (cf. Eq. 9)

$$\mathcal{H}[\rho(r,z)]\mathbf{j}_\kappa = g\kappa(r,z,\varphi)\mathbf{j} \equiv \tilde{\alpha}(-\sin\varphi, \cos\varphi, 0) \tag{14}$$

with

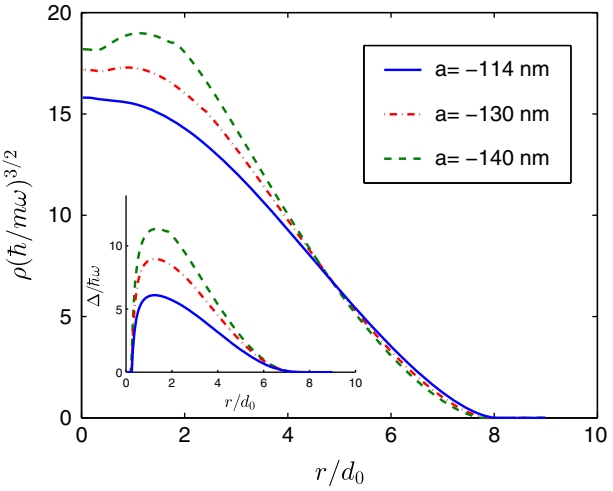

Fig. 3 Density and gap profiles (*inset*) as function of r (in units of d_0) at $z = 0$ and several values of a as indicated in the plot (Color figure online)

$$\mathcal{H}[\rho] = -\frac{\hbar^2\nabla^2}{4m} + 2V(r,z) + \mathrm{g}\rho(r,z) - 2\mu_0, \tag{15}$$

$$\tilde{\alpha}(r,z,\varphi) = \mathrm{g}\kappa(r,z,\varphi)\, j \equiv \alpha(r,z)e^{\imath 2l\varphi}, \tag{16}$$

$$\alpha(r,z) = \mathrm{g}\kappa(r,z)\, j. \tag{17}$$

Equation (14) splits then into cartesian components

$$\mathcal{H}\mathbf{j}_{\kappa x} = -\tilde{\alpha}\sin\varphi, \tag{18}$$

$$\mathcal{H}\mathbf{j}_{\kappa y} = \tilde{\alpha}\cos\varphi, \tag{19}$$

$$\mathcal{H}\mathbf{j}_{\kappa z} = 0. \tag{20}$$

The last of these equations indicates that the z-component of the pair current is either vanishing or just an eigenfunction of the mean field, with eigenvalue μ_0. For the planar components, in correspondence with the choice for the pair density, we look for solutions of the form

$$\mathbf{j}_{\kappa x} = X(r,z,\varphi)e^{\imath 2l\varphi}, \tag{21}$$

$$\mathbf{j}_{\kappa y} = Y(r,z,\varphi)e^{\imath 2l\varphi}. \tag{22}$$

Since the angular Laplacian $\partial^2/\partial\varphi^2$ acting on a product of functions introduces a single derivative, Eqs. (18) and (19) can be solved with the *ansatz*

$$X(r,z,\varphi) = -X_1(r,z)\sin\varphi + \imath X_2(r,z)\cos\varphi, \tag{23}$$

$$Y(r,z,\varphi) = \imath Y_1(r,z)\sin\varphi + Y_2(r,z)\cos\varphi. \tag{24}$$

Introducing (23) into (18) we readily get

$$\mathcal{H}_l X_1 + \frac{\hbar^2 l}{mr^2} X_2 = \alpha, \tag{25}$$

$$\frac{\hbar^2 l}{mr^2} X_1 + \mathcal{H}_l X_2 = 0. \tag{26}$$

Here $\mathcal{H}_l$ is the hamiltonian in (15) plus the centrifugal potential for pairs $\hbar^2 l^2/mr^2$. We note that these equations are compatible with real X_1 and X_2. The same procedure for the y-component yields similar relations with $Y_2 = X_1$ and $Y_1 = X_2$. Accordingly, we can write the planar pair current in the form

$$\mathbf{j}_\kappa = e^{\imath 2l\varphi}(X_1\hat{\varphi} + \imath X_2\hat{r}). \tag{27}$$

This expression shows that in addition to the multipolarity phase factor already imposed into the pairing field $\kappa(r, z, \varphi)$, the pair current is intrinsically complex: while the real part of the amplitude, which could be regarded as the "observable" current, is parallel to the vortex field, there appears a divergent contribution in the radial direction. Before analyzing further the consequences of this imaginary term, we note that in practice, one may bypass the solution of the coupled system (25) and (26) resorting to the quantities $\mathbf{j}_{\kappa\pm} = \mathbf{j}_{\kappa x} \pm \imath \mathbf{j}_{\kappa y}$. Equations (18) and (19) decouple as

$$\mathcal{H}\mathbf{j}_{\kappa\pm} = \pm\imath\tilde{\alpha} e^{\pm\imath\varphi} \tag{28}$$

which is solved by

$$\mathbf{j}_{\kappa\pm} = \pm\imath A_\pm e^{\imath(2l \pm 1)\varphi} \tag{29}$$

with real $A_\pm$ that satisfy

$$\left[\mathcal{H} + \frac{\hbar^2(2l \pm 1)^2}{4mr^2}\right] A_\pm = \alpha. \tag{30}$$

From (29) we can reconstruct the x, y-components as

$$\mathbf{j}_{\kappa x} = \left[-(A_+ + A_-)\sin\varphi + \imath\,(A_+ - A_-)\cos\varphi\right] e^{\imath 2l\varphi}, \tag{31}$$

$$\mathbf{j}_{\kappa y} = \left[(A_+ + A_-)\cos\varphi + \imath\,(A_+ - A_-)\sin\varphi\right] e^{\imath 2l\varphi} \tag{32}$$

from which we recognize the relations $X_1 = A_+ + A_-$ and $X_2 = A_+ - A_-$.

4 Numerical Illustrations

We now discuss some typical current profiles computed with Eqs. (30) to (31). Plots for the real and imaginary parts of the pair current are respectively depicted in the

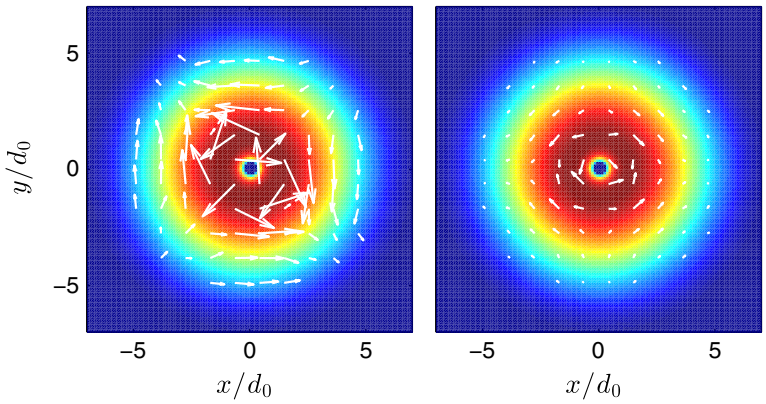

Fig. 4 Plots of the pair current on the (x, y) plane for angular momentum $l = 1$. The background corresponds to contours of the pairing gap Δ. *Left panel* real part. *Right panel* imaginary part (Color figure online)

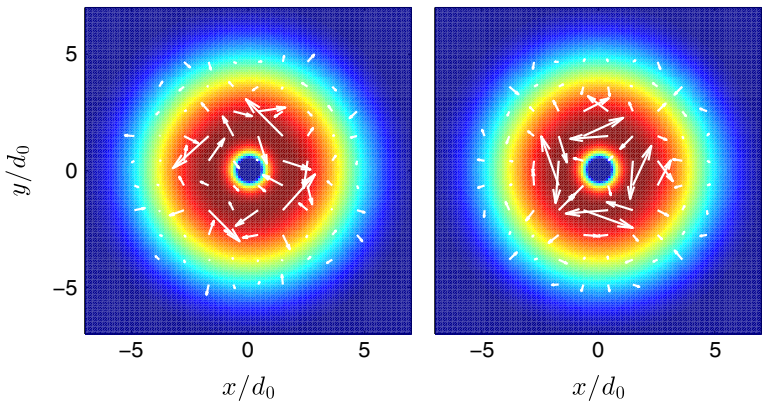

Fig. 5 Same as Fig. 4 for $l = 2$ (Color figure online)

left and right panels of Figs. 4 and 5, in correspondence with Figs. 1 and 2. The φ-dependence of both the real and imaginary components is due to the admixture with the multipolar phase factor and the increasing complexity of the patterns in Fig. 5 reveals the magnitude of the angular momentum. It is interesting as well to consider the relative magnitudes of the currents. This is seen in Fig. 6, where we can appreciate that the value of the imaginary part of $\mathbf{j}_\kappa$ is comparable with the original particle current.

Moreover, as the imposed v_s is increased, the particle current diminishes since the gap is more depleted and therefore fewer particles participate. This is seen in the solid line of the bottom panel in Fig. 6 as compared to the upper panel.

We note here that in the stationary regime, according to (27), Eq. (6) becomes

$$0 = \frac{\rho}{m}\nabla\mu + \frac{4g}{\hbar}\kappa X_2 \hat{\mathbf{r}} \tag{33}$$

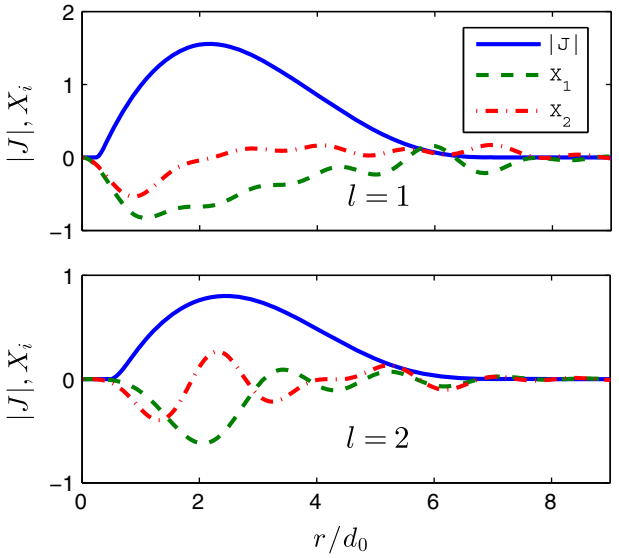

Fig. 6 Modulus of the particle current together with the real and imaginary part of the pair current (removing the phase factor) as functions of the distance to the trap center. *Upper panel* $l = 1$; *lower panel* $l = 2$ (Color figure online)

which expresses the balance between the force proportional to $\nabla\mu$ and the radial drift introduced by the pair current. However, our scheme extracts the density profiles as solutions of the LDA equation (12), which corresponds to disregarding X_2 in (33); this approach can be legitimated a posteriori by the fact that X_2 is of order g. In fact, the calculations illustrated in Fig. 6 show that the magnitude of X_2 remains small compared to the particle current, even for not too low values of the scattering length. Consequently, a perturbation approach permits to estimate the density change relative to the zero-order profiles obtained within STF, by setting $\rho_c = \rho_0 + \delta\rho$ and linearizing Eq. (33). We can visualize the relative size of this correction in Fig. 7, that shows that this correction is practically vanishing for weakly interacting systems as seen in the case $a = -30$ nm. The density shift for $a = -114$ nm can reach a 3 % near the maximum of the dipolar configuration, and becomes stronger for the quadrupole profile. For illustrative purposes we have also included the result for the largest $|a|$ considered, where the corrections can be as large as 25 % at the trap center for the quadrupole configuration. This confirms the expectation that the perturbative approach become less reliable for large couplings when also the mean-field approximation involved in the fluiddynamics starts to be inaccurate. It is worthwhile remarking that the calculation is more demanding for larger l and/or a.

We also mention that it is possible to define the pair velocity $\mathbf{v}_\kappa$ by the relation $\mathbf{j}_\kappa = \kappa\mathbf{v}_\kappa$. Since the φ-dependence of $\kappa(r, z, \varphi)$ is given by the same multipolarity phase factor, the latter is not present in the pair velocity whose form is

$$\mathbf{v}_\kappa = \frac{1}{\kappa(r, z)}(X_1\hat{\varphi} + \imath X_2\hat{r}). \tag{34}$$

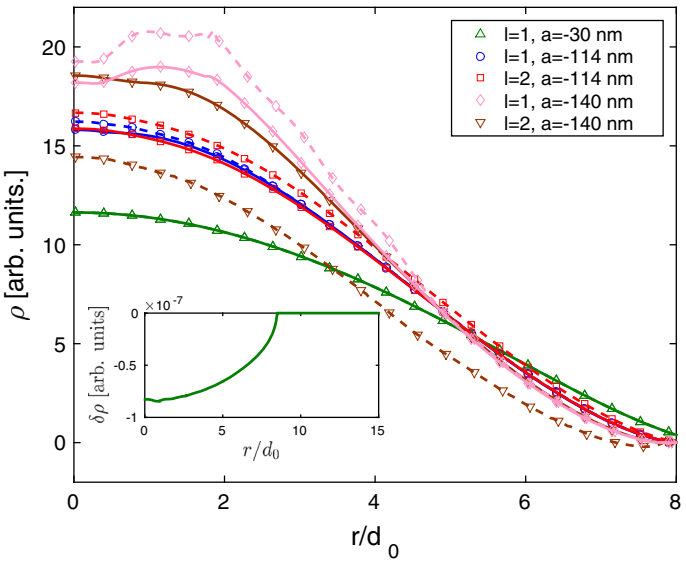

Fig. 7 Original density profile ρ_0 (*solid lines*) and perturbed one ρ_c (*dashed lines*) in the presence of a dipole and a quadrupole vortex for $a = -114$ and -140 nm, and of a dipole for $a = -30$ nm. The *inset* shows the correction $\delta\rho = \rho_c - \rho$ for the case $a = -30$ nm (Color figure online)

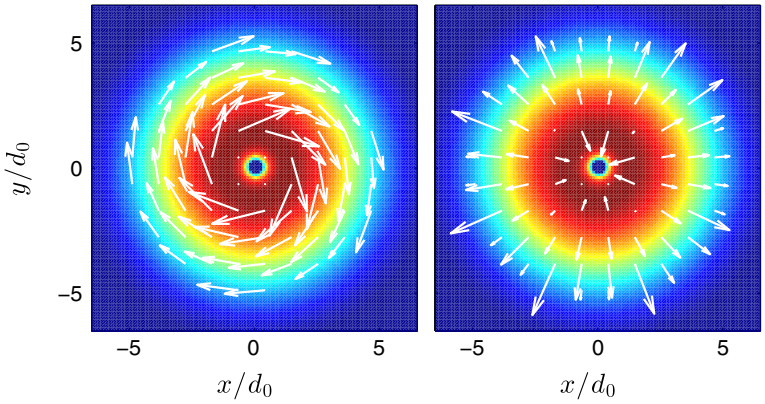

Fig. 8 Same as Fig. 4 for the pair velocity in Eq. (34) (Color figure online)

The pair velocity is illustrated in Figs. 8 and 9 for the dipolar and quadrupolar flows, respectively. The suppression of the phase factor leaves us with a pristine radial drift in the imaginary part, to be contrasted with the angle-dependent pair current in Figs. 4 and 5. Taking advantage of the disappearance of the phase factor, the dynamical equation (6) can be written as

$$\frac{\partial \mathbf{j}}{\partial t} = -\frac{\rho}{m}\nabla\mu - \frac{4g|\kappa|^2}{\hbar}\mathrm{Im}(\mathbf{v}_\kappa). \tag{35}$$

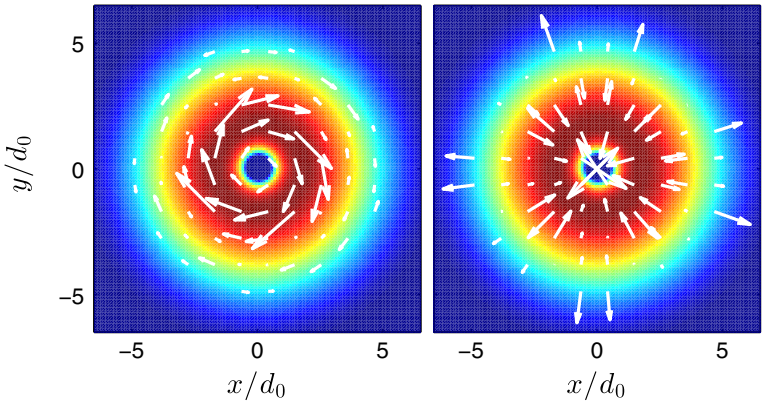

Fig. 9 Same as Fig. 5 for the pair velocity (Color figure online)

Thus, while the real part of the pair velocity simply scales with the particle velocity field, its imaginary term is the source of the additional radial force acting on the particle current that, in a time-dependent scheme, may provide an radial destabilizing drift on the vortex motion. In other words, the solution found by neglecting this imaginary part in Eq. (33) is not a rigorous stationary solution, since even a drift of order g^2 in a weakly interacting system causes it to move radially towards the periphery of the system. We can show that an exact stationary state with a particle current **j** that includes a radial component may exist; in fact, the treatment in Sect. 3 holds in such a case with a complex amplitude $A_{\pm}$. More importantly, to compute the exact stationary solution one needs to solve the coupled equations (5)–(10) at once, with a particle velocity profile distorted with respect to Eq. (11) as an outcome of a much more demanding numerical calculation, that resigns the advantages of the much simpler STF scheme.

5 Conclusions

Fermion fluiddynamics allows one to introduce aspects of the internal structure and motion of pairs as macroscopic fields. This is an outcome of our underlying philosophy that, seeking a fluid description in terms of fields, pursues the quantum nature of the system to a larger extent by introducing gradients in the form of first and second moments of the pair density, in addition to those of the particle density intrinsic to normal fluid hydrodynamics. As a consequence any macroscopic particle current gives rise to a pair current, which in turn contributes to the generation of particle and pair kinetic energy densities. This occurs even in the stationary regime with impressed vorticity, where we can explicitly compute the complex pair current employing zero-order profiles for the particle and pair densities. For this sake, we extended the local density approximation employed in previous versions of FD, to take into account the presence of the superfluid velocity of an impressed vortex in the calculation of both particle density and current profiles. We show that even for not too weak interaction strengths, the imaginary part of the pair current can be regarded as a perturbation on the local density and pair density; however, the ensuing modifications in the vortex

dynamics may include destabilization of the stationary regime due to the appearance of a radial drift.

Experiments with trapped fermions systems along the BCS–BEC crossover, see e.g. [4,33], demonstrated the existence of vortex lattices both on the BEC and on the BCS side of the resonance. The latter are unstable and researchers have been able to measure the lifetime of the array, and to examine quantitatively its dependence with the intensity of the resonance field. An important speculation was put forward by the authors of Ref. [4]: the observed decrease in lifetime as a function of the magnetic field close to resonance could be traced to coupling of the motion of the loosely bound pairs to their internal motion. We believe that our theory supports this speculation, since we are providing a formal description of one such coupling. As the pair current is essentially the gradient of the pair density, which decreases towards the periphery of the cloud, the real part of the current is, to some extent, an indication of the tendency of the pairs to decouple locally; in this context, the additional force in the particle current gives, in a local description, a drift towards those trap regions of reduced number of pairs where vorticity cannot be supported. This effect is far from trivial, since such a dragging force is not contemplated in the traditional superfluid hydrodynamics.

Another possibility to extract some information about the existence of the dragging force can be traced to the so-called universal character—i.e., independent of statistics—of vortex formation and localization reported in Refs. [35,36]. From our viewpoint, since the pair current is intrinsic to fermion statistics, the evolution pattern of the released fermion and boson clouds containing vortex lattices of the same size, built under similar conditions, should exhibit differences in their lifetimes. Experiments along this line, exploring the evolution of the respective particle densities and vortex lattices in a ballistic expansion, or even in situ, could give indications of the existence of this radial force. In any case, one should keep in mind that the present—simplified—theory applies to a single vortex localized at the trap center, while both in actual experiments [4,33] and theoretical predictions [34] vortices appear in lattices, that evolve as the trap is released and the fermions are driven into a resonant regime from the BCS to the BEC phase [33]. Consequently, the effects here predicted may be enhanced in actual experiments where many vortices are involved, and hence our study can be useful as a starting point; possible initial approaches for theoretical developments that could inspire future experiments, could be to consider two singly quantized vortices in vortex–vortex or vortex–antivortex configurations, as it has been investigated in the case of trapped bosons.

In the present stage, the relation of the pair current to the orbital current of paired fermions remains an open issue. It is worthwhile recalling that the microscopic description of the pair current in terms of the standard Bogoliubov-de-Gennes transformation permits to view this macroscopic field as an average of particle velocities weighted with the pair density, rather than with the particle density [19]. In this respect the pair current cannot be related to the intrinsic angular momentum density in an obvious manner. Its existence may show up in the more strongly interacting systems through a moderate flattening of the peak of the equilibrium density patterns, as well as in vortex dynamics.

Acknowledgments This work was performed under grants PIP 0546 from CONICET, Argentina, PICT 2008-0682 from ANPCYT, Argentina and UBACYT 01/K156 from University of Buenos Aires.

Appendix: The Homogeneous Gas with a Superfluid Velocity

Following [31] we calculate the properties of the homogeneous gas, in particular the particle density, particle current, kinetic energy and all other equilibrium quantities in the presence of a superfluid velocity $\mathbf{v}_s$.

From the BCS equations, the quasiparticle energy spectrum in the case of a uniform superflow for $\tilde{\mu} = \mu - g\rho/2$ is given by

$$E_{\mathbf{k}} = \frac{\hbar^2}{m}\mathbf{k}\cdot\mathbf{q} + \sqrt{\Delta^2 + \left(\varepsilon_k + \frac{\hbar^2 q^2}{2m}\right)^2}, \tag{36}$$

with the superfluid velocity $\mathbf{v}_s = \hbar\mathbf{q}/m$, $\varepsilon_k = \hbar^2 k^2/2m - \tilde{\mu}$, and Δ the gap amplitude. This expression arises from the fact that the BCS amplitudes $u_{\mathbf{k}}$ and $v_{\mathbf{k}}$ acquire respective phases $e^{-\imath\mathbf{q}\cdot\mathbf{r}}$ and $e^{\imath\mathbf{q}\cdot\mathbf{r}}$ in order to account for the phase of the field operators. The BCS procedure then gives

$$\begin{aligned} |u_{\mathbf{k}}|^2 &= \frac{(E_{\mathbf{k}} + \varepsilon_{\mathbf{k}-\mathbf{q}})^2}{\Delta^2 + (E_{\mathbf{k}} + \varepsilon_{\mathbf{k}-\mathbf{q}})^2}, \\ |v_{\mathbf{k}}|^2 &= \frac{\Delta^2}{\Delta^2 + (E_{\mathbf{k}} + \varepsilon_{\mathbf{k}-\mathbf{q}})^2} \end{aligned} \tag{37}$$

and the regularized gap equation reads [30]

$$1 = -\frac{g}{2}\int\left[\frac{u_{\mathbf{k}}v_{\mathbf{k}}}{\Delta}\left(1 - 2\Theta(-E_{\mathbf{k}})\right) - \frac{1}{\hbar^2 k^2/m}\right]\frac{d^3k}{(2\pi)^3}, \tag{38}$$

where Θ is the Heaviside function. For each value of q, we can then compute both the particle density and the particle current as

$$\rho = \int\left[|v_{\mathbf{k}}|^2 + \Theta(-E_{\mathbf{k}})\left(|u_{\mathbf{k}}|^2 - |v_{\mathbf{k}}|^2\right)\right]\frac{d^3k}{(2\pi)^3}, \tag{39}$$

$$\mathbf{j} = \frac{\hbar\mathbf{q}}{m}\rho + \frac{\hbar\mathbf{q}}{m}\int\frac{\mathbf{k}\cdot\mathbf{q}}{q^2}\left[\left(|u_{\mathbf{k}}|^2 + |v_{\mathbf{k}}|^2\right)\Theta(-E_{\mathbf{k}}) - |v_{\mathbf{k}}|^2\right]\frac{d^3k}{(2\pi)^3}, \tag{40}$$

and the Fermi energy ε_F appearing in Eq. (12) is evaluated in terms of intermediate derivatives and current quantities as

$$\varepsilon_F = \frac{3}{5}\tilde{\mu} + \frac{\partial\tilde{\mu}}{\partial\rho}\left(\frac{3}{5}\rho - \frac{2}{5}\frac{\Delta^2}{g\tilde{\mu}}\frac{3g\rho - 2\tilde{\mu}}{\Delta^2 2\tilde{\mu} + 3g/\rho}\right). \tag{41}$$

In the present version of the local density approximations, we first solve the coupled integral Eqs. (38) and (39) for given ρ and q and obtain the gap Δ and μ. Once this is done we compute $\mathbf{j}$ and ε_{F} from Eqs. (40) and (41), that replace the integral equations for gap and particle density in Ref. [30]. While in this reference the integrals over momentum variables are closed in terms of Legendre functions, the angular domains in this case set borders for the integration domain and prevent analytical results; in other words, the integrals in (37) and (38) must be performed numerically for each selection of parameters.

References

1. D. Vollhardt, P. Wölfle, *The Superfluid Phases of Helium 3* (Taylor and Francis, London, 1990)
2. R.J. Donnelly, *Quantized Vortices in Helium II* (Cambridge University Press, Cambridge, 1991)
3. C.F. Barenghi, *Quantized Vortex Dynamics and Superfluid Turbulence* (Springer, New York, 2001)
4. M.W. Zwierlein, J.R. Abo-shaer, A. Schirotzek, C.H. Schunck, W. Ketterle, Nature **435**, 1035 (2005)
5. M.C. Cross, J. Low Temp. Phys. **21**, 525 (1975)
6. M.C. Cross, J. Low Temp. Phys. **26**, 165 (1977)
7. C.R. Hu, W.M. Saslow, Phys. Rev. Lett. **38**, 605 (1977)
8. N.D. Mermin, P. Muzikar, Phys. Rev. B **21**, 980 (1980)
9. H.E. Hall, Phys. Rev. Lett. **54**, 205 (1985)
10. F. Gaitan, Ann. Phys. **235**, 390 (1994)
11. P. Nozières, D. Pines, *The Theory of Quantum Liquids: Superfluid Bose Liquids* (Addison Wesley, New York, 1990)
12. F. Dalfovo, S. Giorgini, L.P. Pitaevskii, S. Stringari, Rev. Mod. Phys. **71**, 463 (1999)
13. P. Ring, P. Schuck, *The Nuclear Many Body Problem* (Springer, Berlin, 1980)
14. M. Di Toro, V.M. Kolomietz, Z. Phys. A **328**, 285 (1987)
15. P. Capuzzi, E.S. Hernández, L. Szybisz, Phys. Rev. A **78**, 043619 (2008)
16. P.W. Anderson, Phys. Rev. **112**, 1900 (1958)
17. N.N. Bogoliubov, Sov. Phys. JETP **34**, 41 (1958)
18. E.S. Hernández, P. Capuzzi, L. Szybisz, J. Low Temp. Phys. **162**, 274 (2011)
19. P. Capuzzi, E.S. Hernández, L. Szybisz, J. Low Temp. Phys. **166**, 242 (2012)
20. P. Capuzzi, E.S. Hernández, L. Szybisz, J. Low Temp. Phys **169**, 362 (2013)
21. S. Giorgini, L.P. Pitaevskii, S. Stringari, Rev. Mod. Phys. **80**, 1215 (2008)
22. P. Capuzzi, E.S. Hernández, L. Szybisz, Eur. Phys. J. D **60**, 347 (2010)
23. E.S. Hernández, P. Capuzzi, L. Szybisz, J. Low Temp. Phys. **162**, 281 (2011)
24. W.D. Phillips, Rev. Mod. Phys. **70**, 721 (1998)
25. B. DeMarco, D.S. Jin, Science **225**, 5434 (1999)
26. C.N. Cohen-Tannoudji, Rev. Mod. Phys. **70**, 707 (1998)
27. R. Sensarma, M. Randeria, T.-L. Ho, Phys. Rev. Lett. **96**, 090403 (2006)
28. N. Fukushima, Y. Ohashi, E. Taylor, A. Griffin, Phys. Rev. A **75**, 033609 (2007)
29. S. Simonucci, P. Pieri, G.C. Strinati, Phys. Rev. B **87**, 214507 (2013)
30. T. Papenbrock, G.F. Bertsch, Phys. Rev. C **59**, 2052 (1999)
31. P.G. De Gennes, *Superconductivity of Metals and Alloys* (Westview Press, Boulder, 1999)
32. E.R.I. Abraham, W.I. McAlexander, J.M. Gerton, R.G. Hulet, R. Ct, A. Dalgarno, Phys. Rev. A **55**, R3299 (1997)
33. C.H. Schunck, M.W. Zwierlein, A. Schirotzek, W. Ketterle, Phys. Rev. Lett. **98**, 050404 (2007)
34. G. Tonini, F. Werner, Y. Castin, Eur. Phys. J. D **39**, 283 (2006)
35. M. Toreblad, M. Borgh, M. Koskinen, M. Manninen, S.M. Reimann, Phys. Rev. Lett. **93**, 090407 (2004)
36. S.M. Reinmann, M. Koskinen, Y. Yu, M. Mannien, Phys. Rev. A **74**, 043603 (2006)